

Atom interferometry with Bose-Einstein condensates in a double-well potential

Y. Shin, M. Saba, T. A. Pasquini, W. Ketterle, D. E. Pritchard, and A. E. Leanhardt*

Department of Physics, MIT-Harvard Center for Ultracold Atoms, and Research Laboratory of Electronics, Massachusetts Institute of Technology, Cambridge, Massachusetts, 02139

(Dated: March 22, 2002)

A trapped-atom interferometer was demonstrated using gaseous Bose-Einstein condensates coherently split by deforming an optical single-well potential into a double-well potential. The relative phase between the two condensates was determined from the spatial phase of the matter wave interference pattern formed upon releasing the condensates from the separated potential wells. Coherent phase evolution was observed for condensates held separated by $13\ \mu\text{m}$ for up to 5 ms and was controlled by applying ac Stark shift potentials to either of the two separated condensates.

PACS numbers: 03.75.Dg, 39.20.+q, 03.75.-b, 03.75.Lm

Demonstrating atom interferometry with particles confined by magnetic [1, 2, 3, 4] and optical [5] microtraps and waveguides would realize the matter wave analog of optical interferometry using fiber-optic devices. Current proposals for confined-atom interferometers rely on the merger and separation of two potential wells to coherently divide atomic wavepackets [6, 7, 8]. This type of division differs from previously demonstrated atomic beam splitters. To date, atomic beams and vapors have been coherently diffracted into different momentum states by mechanical [9, 10] and optical [11] gratings, and Bose-Einstein condensates have been coherently delocalized over multiple sites in optical lattices [12, 13, 14, 15, 16, 17]. Atom interferometers utilizing these beam splitting elements have been used to sense accelerations [12, 18] and rotations [19, 20], monitor quantum decoherence [21], characterize atomic and molecular properties [22], and measure fundamental constants [18, 23].

In this Letter, we demonstrate a trapped-atom interferometer with gaseous Bose-Einstein condensates confined in an optical double-well potential. Condensates were coherently split by deforming an initially single-well potential into two wells separated by $13\ \mu\text{m}$. The relative phase between the two condensates was determined from the spatial phase of the matter wave interference pattern formed upon releasing the atoms from the separated potential wells [17, 24]. This recombination method avoids deleterious mean field effects [25, 26] and detects applied phase shifts on a single realization of the experiment, unlike in-trap recombination schemes [6, 7, 8].

The large separation between the split potential wells allowed the phase of each condensate to evolve independently and either condensate to be addressed individually. An ac Stark phase shift was applied to either condensate by temporarily turning off the optical fields generating its potential well. The spatial phase of the resulting matter wave interference pattern shifted linearly with the applied phase shift and was independent of the time of its application. This verified the phase sensitivity of the interferometer and the independent phase evolution

of the separated condensates. The measured coherence time of the separated condensates was 5 ms.

The present work demonstrates a trapped-atom interferometer with two interfering paths. This geometry has the flexibility to measure either highly localized potentials or uniform potential gradients, such as those arising from atom-surface interactions or the earth's gravitational field, respectively. In contrast, multiple-path interferometers demonstrated in optical lattice systems are restricted to measurements of the latter [12, 17].

Bose-Einstein condensates containing over $10^7\ ^{23}\text{Na}$ atoms were created in the $|F = 1, m_F = -1\rangle$ state in a magnetic trap, captured in the focus of a 1064 nm optical tweezers laser beam, and transferred into an auxiliary "science" chamber as described in Ref. [27]. In the science chamber, the condensate was loaded from the optical tweezers into the interferometer's single-well optical trap formed by a counter-propagating, orthogonally-polarized 1064 nm laser beam shifted in frequency from the tweezers by $\sim 100\ \text{MHz}$ to avoid interference effects.

A schematic diagram of the setup for the interferometer's optical trap is shown in Fig. 1(a). The optical potentials were derived from a collimated laser beam that passed through an acousto-optic modulator (AOM) and was focused onto the condensate with a lens. The AOM was driven by two radio frequency (rf) signals to create the double-well potential. The separation between the potential wells was controlled by the frequency difference between the rf drives. The $1/e^2$ radius of each focused beam was $5\ \mu\text{m}$. For typical optical powers, this resulted in a single beam trap depth $U_0 = h \times 5\ \text{kHz}$, where h is Planck's constant, and a radial (axial) trap frequency $f_r = 615\ \text{Hz}$ ($f_z = 30\ \text{Hz}$).

The condensate was initially loaded into the single-well trap shown in Fig. 1(b). After holding the cloud in this trap for 15 s to damp excitations, the peak atomic mean field energy was $\tilde{\mu}_0 \approx h \times 3\ \text{kHz}$. The single-well trap was deformed into the double-well potential shown in Fig. 1(c) by linearly increasing the frequency difference between the rf signals driving the AOM in 5 ms. The amplitude of the rf signals were tailored during the splitting

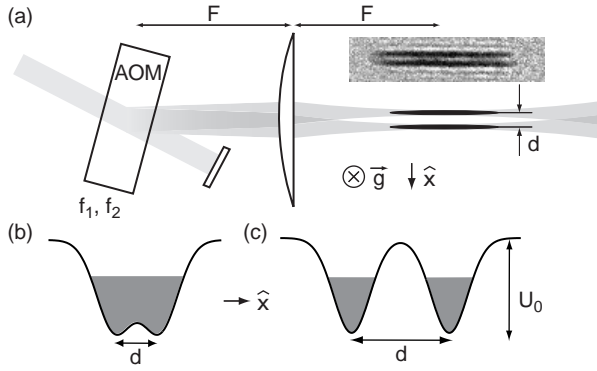


FIG. 1: (a) Schematic diagram of the optical setup for the double-well potential. An acousto-optic modulator (AOM) was driven by two frequencies, f_1 and f_2 , and diffracted a collimated beam into two beams. The AOM was placed in the focal plane of a lens of focal length F so that the two beams propagated parallel to each other. The radial separation of the potential wells, d , was controlled by the frequency difference, $\Delta f = |f_1 - f_2|$. \vec{g} denotes the direction of gravitational acceleration. The absorption image shows two well-separated condensates confined in the double-well potential diagrammed in (c). The field of view is $70 \mu\text{m} \times 300 \mu\text{m}$. Energy diagrams for (b) initial single-well trap with $d = 6 \mu\text{m}$ and (c) final double-well trap with $d = 13 \mu\text{m}$. In both (b) and (c), $U_0 = h \times 5 \text{ kHz}$ and the peak atomic mean field energy was $\sim h \times 3 \text{ kHz}$. The potential “dimple” in (b) was $< h \times 500 \text{ Hz}$ which was much less than the peak atomic mean field energy allowing the trap to be characterized as a single-well. The potential “barrier” in (c) was $h \times 4.7 \text{ kHz}$ which was larger than the peak atomic mean field energy allowing the resulting split condensates to be characterized as independent.

process to guarantee an even division of the condensate atoms and nearly equal trap depths after splitting.

The key achievement of this work was the reproducibility of the spatial phase of the matter wave interference pattern on each realization of the experiment. Figure 2 shows a typical matter wave interference pattern formed by the condensates released from the double-well potential. The reproducibility directly confirmed that deforming the optical potential from a single-well into a double-well coherently split the condensate into two clouds with deterministic relative phase. While past work suffered from an unstable potential barrier separating the two condensates and irreproducible turn off a high current magnetic trap to initiate ballistic expansion [24], the current experiment derived its double-well potential from a single laser beam. Thus, vibrations and fluctuations of the laser beam were common-mode to both wells and a clean and rapid trap turn off was achieved.

The condensates were sufficiently separated that their phases evolved independent of each other to the extent that no coupling between the potential wells could be detected. This claim is supported qualitatively by the absorption image in Fig. 1(a) and the observation of high-

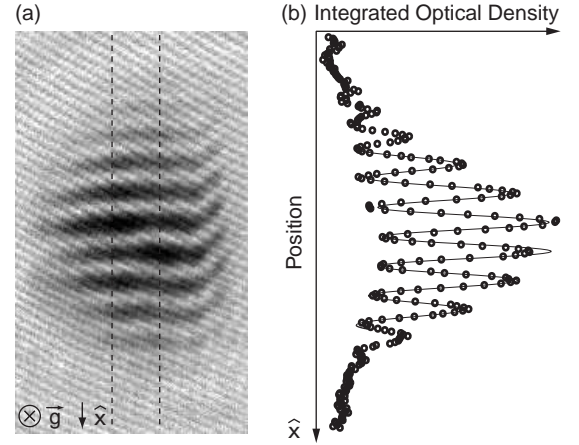


FIG. 2: Matter wave interference. (a) Absorption image of condensates released from the double-well potential in Fig. 1(c) and allowed to overlap during 30 ms of ballistic expansion. The imaging axis was parallel to the direction of gravitational acceleration, \vec{g} . The field of view is $600 \mu\text{m} \times 350 \mu\text{m}$. (b) Radial density profiles were obtained by integrating the absorption signal between the dashed lines, and typical images gave $> 60\%$ contrast. The solid line is a fit to a sinusoidally-modulated Gaussian curve from which the phase of the interference pattern was extracted (see text).

contrast matter wave interference patterns that penetrated the full atomic density profile with uniform spatial period and no thick central fringe [28], and quantitatively by measurements of the phase evolution (Figs. 3 and 4).

The relative phase between the two separated condensates was determined by the spatial phase of their matter wave interference pattern. For a ballistic expansion time $t \gg 1/f_r$, each condensate had a quadratic phase profile [29], $\psi_{\pm}(\vec{r}, t) = \sqrt{n_{\pm}(\vec{r}, t)} \exp(i \frac{m}{2\hbar t} |\vec{r} \pm \vec{d}/2|^2 + \phi_{\pm})$, where \pm denotes one well or the other, n_{\pm} is the condensate density, $\hbar = h/2\pi$, m is the atomic mass, and ϕ_{\pm} is the condensate phase. This resulted in a total density profile for the matter wave interference pattern

$$n(\vec{r}, t) = (n_+ + n_- + 2\sqrt{n_+ n_-} \cos(\frac{m\vec{d}}{\hbar t} \cdot \vec{r} + \phi_r)), \quad (1)$$

where $\phi_r = \phi_+ - \phi_-$ is the relative phase between the two condensates and $\vec{d} = d\hat{x}$. To extract ϕ_r , the integrated cross section shown in Fig. 2(b) was fit with a sinusoidally-modulated Gaussian curve, $G(x) = A \exp(-(x - x_c)^2/\sigma^2) (1 + B \cos(\frac{2\pi}{\lambda}(x - x_0) + \phi_f))$, where ϕ_f is the phase of the interference pattern with respect to a chosen fixed x_0 . Ideally, if x_0 was set at the center of the two wells, then $\phi_r = \phi_f$. However, misalignment of the imaging axis with the direction of gravitational acceleration created a constant offset, $\phi_f = \phi_r + \delta\phi$. With $t = 30 \text{ ms}$ the measured fringe period, $\lambda = 41.5 \mu\text{m}$, was within 4% of the point source formula prediction [Eq. (1)], $\hbar t/m d = 39.8 \mu\text{m}$.

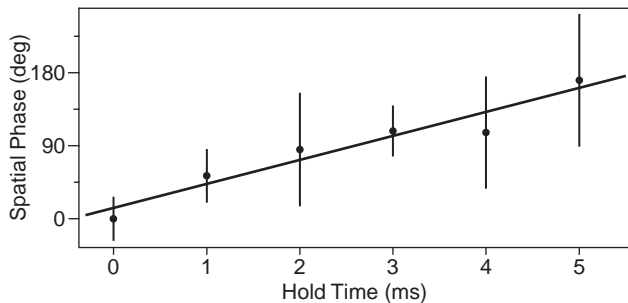


FIG. 3: Phase coherence of the separated condensates. The spatial phase of the interference pattern is plotted versus hold time after splitting. Each point represents the average of eight measurements, and the error bars are \pm one standard deviation. The phase evolution was due to unequal trap depths for the two wells, which was determined from the linear fit to be $h \times 70$ Hz or $\sim 1\%$ of the trap depth.

The coherent phase evolution of the split condensates is displayed quantitatively in Figs. 3 and 4. The relative phase, ϕ_r , between the separated condensates was observed to evolve linearly in time and the standard deviation of eight measurements of ϕ_f was < 90 degrees up to 5 ms after splitting (Fig. 3). Furthermore, for hold times between 0 and 1 ms, the standard deviation was substantially smaller, < 40 degrees. Since ϕ_r distributed randomly between -180 and $+180$ degrees would have a standard deviation of ~ 104 degrees, the results in Figs. 3 and 4 clearly demonstrate that the separated condensates had a reproducible relative phase after splitting. The linear time evolution of ϕ_r was due to a chemical potential difference between separated condensates and could be controlled by varying the trap depths of the individual potential wells after splitting.

Fundamental limits on the phase coherence between isolated condensates arise due to Poissonian number fluctuations associated with the coherent state description of the condensate [30, 31, 32]. For our experimental parameters, the time scale for phase diffusion was ~ 200 ms. The uncertainty in determining ϕ_f at longer hold times > 5 ms is attributed to axial and breathing-mode excitations created during the splitting process. These excitations lead to interference fringes that were angled and had substantial curvature, rendering a determination of ϕ_f impossible. Splitting the condensate more slowly in an effort to minimize excitations, but still fast compared to the phase diffusion time, did not improve the measured stability of ϕ_f . Since controlling axial excitations appears critical for maintaining phase coherence, splitting condensates that are freely propagating in a waveguide potential may be more promising [3].

The phase sensitivity of the trapped-atom interferometer was demonstrated by applying ac Stark phase shifts to either (or both) of the two separated condensates. Phase shifts were applied to individual condensates by

pulsing off the optical power generating the corresponding potential well for a duration $\tau_p \ll 1/f_r$. Figure 4(a) shows that the spatial phase of the matter wave interference pattern shifted linearly with the pulse duration, as expected. Due to the inhomogeneous optical potential, $U(r)$, the applied ac Stark phase shifts varied across the condensate as $\Delta\phi(r) = -U(r)\tau_p/\hbar$. Averaging this phase shift over the inhomogeneous condensate density, $n(\vec{r})$, approximates the expected spatial phase shift of the matter wave interference pattern as $\Delta\phi = \frac{1}{N} \int d^3\vec{r} n(\vec{r}) \Delta\phi(\vec{r}) = (U_0 - \frac{2}{7}\bar{\mu}_0)\Delta t/\hbar$, where N is the number of atoms, and U_0 and $\bar{\mu}_0$ are the trap depth and mean field energy at the center of each potential well, respectively. The measured phase shifts yielded $U_0 = h \times 5$ kHz [Fig. 4(b)], which was consistent with calculations based on other measured trap parameters.

The measured phase shifts of the matter wave interference depended only on the time-integral of the applied ac Stark phase shifts [Fig. 4(b)], as expected for uncoupled condensates. The final relative phase, ϕ_r , should be the same on different phase trajectories because the history of phase accumulation does not affect the total amount of accumulated phase. For coupled condensates, Josephson oscillations between the wells would cause the relative phase to vary nonlinearly with time [25, 29] and produce a time dependent signal in Fig. 4(b). Due to the large well separation and mean field energy $h \times 1.7$ kHz below the barrier height, the single-particle tunnelling rate in our system was extremely low ($\lesssim 10^{-3}$ Hz) [29], and the condensates were effectively uncoupled.

In conclusion, we have performed atom interferometry with Bose-Einstein condensates confined in an optical double-well potential. A coherent condensate beam splitter was demonstrated by deforming a single-well potential into a double-well potential. The large spatial separation between the potential wells guaranteed that each condensate evolved independently and allowed for addressing each condensate individually. Recombination was performed by releasing the atoms from the double-well potential and allowing them to overlap while expanding ballistically. Implementing a similar readout scheme with magnetic potentials generated by microfabricated current carrying wires should be possible and would eliminate deleterious mean field effects inherent in proposals using in-trap wavepacket recombination. Propagating the separated condensates along a waveguide prior to phase readout would create an atom interferometer with an enclosed area, and hence with rotation sensitivity.

We thank W. Jhe, C. V. Nielsen, and A. Schirotzek for experimental assistance and S. Gupta, Z. Hadzibabic, and M. W. Zwierlein for critical comments on the manuscript. This work was funded by ARO, NSF, ONR, and NASA. M.S. acknowledges additional support from the Swiss National Science Foundation.

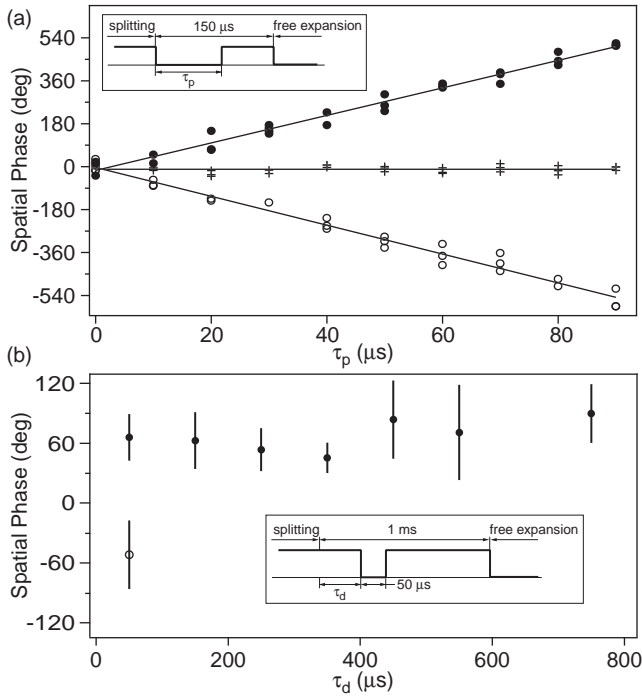


FIG. 4: Trapped-atom interferometry. (a) ac Stark phase shifts were applied to either well exclusively (solid circles and open circles) or both wells simultaneously (crosses) by turning off the corresponding rf signal(s) driving the AOM for a duration τ_p . The resulting spatial phase of the matter wave interference pattern scaled linearly with τ_p and hence the applied phase shift. Applying the ac Stark shift to the opposite well (solid versus open circles) resulted in an interference pattern phase shift with opposite sign. Applying ac Stark shifts to both wells (crosses) resulted in no phase shift for the interference pattern. This data was taken with a slightly modified experimental setup such that the trap depth of the individual potential wells was $U_0 = h \times 17$ kHz. (b) A $50 \mu\text{s}$ pulse induced a 70 degree shift independent of the pulse position. The experimental setup was as described in Fig. 1. Solid and open circles have the same meaning as in (a). The insets show the time sequence of the optical intensity for the well(s) temporarily turned off.

* URL: http://cua.mit.edu/ketterle_group/

- [1] H. Ott, J. Fortagh, G. Schlotterbeck, A. Grossmann, and C. Zimmermann, Phys. Rev. Lett. **87**, 230401 (2001).
- [2] W. Hänsel, P. Hommelhoff, T. W. Hänsch, and J. Reichel, Nature **413**, 498 (2001).
- [3] A. E. Leanhardt, A. P. Chikkatur, D. Kielpinski, Y. Shin, T. L. Gustavson, W. Ketterle, and D. E. Pritchard, Phys. Rev. Lett. **89**, 040401 (2002).
- [4] S. Schneider, A. Kasper, C. vom Hagen, M. Bartenstein, B. Engeser, T. Schumm, I. Bar-Joseph, R. Folman, L. Feenstra, and J. Schmiedmayer, Phys. Rev. A **67**, 023612 (2003).
- [5] R. Dumke, T. Muther, M. Volk, W. Ertmer, and G. Birkl,

- Phys. Rev. Lett. **89**, 220402 (2002).
- [6] E. A. Hinds, C. J. Vale, and M. G. Boshier, Phys. Rev. Lett. **86**, 1462 (2001).
- [7] W. Hänsel, J. Reichel, P. Hommelhoff, and T. W. Hänsch, Phys. Rev. A **64**, 063607 (2001).
- [8] E. Andersson, T. Calarco, R. Folman, M. Andersson, B. Hessmo, and J. Schmiedmayer, Phys. Rev. Lett. **88**, 100401 (2002).
- [9] O. Carnal and J. Mlynek, Phys. Rev. Lett. **66**, 2689 (1991).
- [10] D. W. Keith, C. R. Ekstrom, Q. A. Turchette, and D. E. Pritchard, Phys. Rev. Lett. **66**, 2693 (1991).
- [11] M. Kasevich and S. Chu, Phys. Rev. Lett. **67**, 181 (1991).
- [12] B. P. Anderson and M. A. Kasevich, Science **282**, 1686 (1998).
- [13] C. Orzel, A. K. Tuchman, M. L. Fenselau, M. Yasuda, and M. A. Kasevich, Science **291**, 2386 (2001).
- [14] F. S. Cataliotti, S. Burger, C. Fort, P. Maddaloni, F. Minardi, A. Trombettoni, A. Smerzi, and M. Inguscio, Science **293**, 843 (2001).
- [15] M. Greiner, I. Bloch, O. Mandel, T. W. Hänsch, and T. Esslinger, Phys. Rev. Lett. **87**, 160405 (2001).
- [16] M. Greiner, O. Mandel, T. Esslinger, T. W. Hänsch, and I. Bloch, Nature **415**, 39 (2002).
- [17] O. Mandel, M. Greiner, A. Widera, T. Rom, T. W. Hänsch, and I. Bloch, Phys. Rev. Lett. **91**, 010407 (2003).
- [18] A. Peters, K. Y. Chung, B. Young, J. Hensley, and S. Chu, Phil. Trans. R. Soc. Lond. A **355**, 2223 (1997).
- [19] A. Lenef, T. D. Hammond, E. T. Smith, M. S. Chapman, R. A. Rubenstein, and D. E. Pritchard, Phys. Rev. Lett. **78**, 760 (1997).
- [20] T. L. Gustavson, P. Bouyer, and M. A. Kasevich, Phys. Rev. Lett. **78**, 2046 (1997).
- [21] M. S. Chapman, T. D. Hammond, A. Lenef, J. Schmiedmayer, R. A. Rubenstein, E. Smith, and D. E. Pritchard, Phys. Rev. Lett. **75**, 3783 (1995).
- [22] C. R. Ekstrom, J. Schmiedmayer, M. S. Chapman, T. D. Hammond, and D. E. Pritchard, Phys. Rev. A **51**, 3883 (1995).
- [23] S. Gupta, K. Dieckmann, Z. Hadzibabic, and D. E. Pritchard, Phys. Rev. Lett. **89**, 140401 (2002).
- [24] M. R. Andrews, C. G. Townsend, H.-J. Miesner, D. S. Durfee, D. M. Kurn, and W. Ketterle, Science **275**, 637 (1997).
- [25] A. Smerzi, S. Fantoni, S. Giovanazzi, and S. R. Shenoy, Phys. Rev. Lett. **79**, 4950 (1997).
- [26] J. A. Stickney and A. A. Zozulya, Phys. Rev. A **66**, 053601 (2002).
- [27] T. L. Gustavson, A. P. Chikkatur, A. E. Leanhardt, A. Görlitz, S. Gupta, D. E. Pritchard, and W. Ketterle, Phys. Rev. Lett. **88**, 020401 (2002).
- [28] A. Röhl, M. Naraschewski, A. Schenzle, and H. Wallis, Phys. Rev. Lett. **78**, 4143 (1997).
- [29] F. Dalfovo, S. Giorgini, L. P. Pitaevskii, and S. Stringari, Rev. Mod. Phys. **71**, 463 (1999).
- [30] M. Lewenstein and L. You, Phys. Rev. Lett. **77**, 3489 (1996).
- [31] J. Javanainen and M. Wilkens, Phys. Rev. Lett. **78**, 4675 (1997).
- [32] C. Menotti, J. R. Anglin, J. I. Cirac, and P. Zoller, Phys. Rev. A **63**, 023601 (2001).